PCCP

PAPER

View Article Online
View Journal | View Issue

Cite this: *Phys. Chem. Chem. Phys.*, 2017, **19**, 17677

Fast crystalline ice formation at extremely low temperature through water/neon matrix sublimation†

Tetsuya Hama, *[a] Shinnosuke Ishizuka,[a] Tomoya Yamazaki,[a] Yuki Kimura,[a] Akira Kouchi,[a] Naoki Watanabe,[a] Toshiki Sugimoto[bc] and Valerio Pirronello[d]

Received 18th May 2017,
Accepted 16th June 2017

DOI: 10.1039/c7cp03315j

rsc.li/pccp

Crystalline ice formation requires water molecules to be sufficiently mobile to find and settle on the thermodynamically most stable site. Upon cooling, however, diffusion and rearrangement become increasingly kinetically difficult. Water ice grown by the condensation of water vapor in laboratory is thus generally assumed to be in a metastable amorphous form below 100 K. Here, we demonstrate the possibility of crystalline ice formation at extremely low temperature using a water/neon matrix (1/1000, 30 000 monolayers) prepared at 6 K, which is subsequently warmed to 11–12 K. *In situ* infrared spectroscopy revealed the assembly of the dispersed water molecules, forming crystalline ice I during the sublimation of the neon matrix for 40–250 seconds. This finding indicates that the high mobility of the water molecules during matrix sublimation can overcome the kinetic barrier to form crystals even at extremely low temperature.

Introduction

Water exhibits a rich variety of solid forms. Seventeen crystalline phases have so far been discovered experimentally: two forms of ice I (*i.e.*, hexagonal ice I_h and cubic ice I_c) and ice II–XVI.[1,2] This unique polymorphism stems from hydrogen-bonding networks that are sensitive to pressure and temperature. At low temperatures, however, amorphous ice without any long-range ordered structure is generated.[3–6] For example, water vapor deposition on a substrate below 100 K usually results in amorphous ice: the impinging water molecules readily create hydrogen bonds with the ice surface before they can diffuse to the energetically most-favorable crystalline sites.[7] Because the activation barrier for rearrangement of the hydrogen-bonding network is 60 ± 10 kJ mol^{-1},[8,9] amorphous ice can become crystalline within laboratory timescales only at temperatures above 130 K.[8,10] Crystallisation below 60 K would take much longer than the age of the universe.[10] For example, cosmic dust grains, the precursors of planetary materials, remain covered with amorphous ice in cold interstellar clouds at 10–20 K during their lifetimes of tens of million years.[11,12] The formation of crystalline ice at extremely low temperature has thus been implicitly precluded.

This study reports the formation of crystalline water ice at 11–12 K. We prepared a water/neon matrix (H_2O/Ne = 1/1000) at 6 K in a vacuum environment, in which H_2O molecules were dispersed in a Ne crystal. The matrix was then warmed to 11–12 K to let the Ne atoms sublime. *In situ* infrared (IR) spectroscopy revealed that the dispersed H_2O molecules assembled while the Ne atoms sublimed, forming a long-range ordered crystalline hydrogen-bonding network.

Experimental methods

The experimental apparatus comprised a main ultrahigh vacuum chamber (base pressure 10^{-8} Pa), an Al substrate mounted on the cold head of a closed-cycle He refrigerator, and a Fourier transform infrared spectrometer (FT-IR).[13] The apparatus is essentially identical to that of our previous study.[14,15] The temperature of the Al substrate was measured using a Si-diode sensor (DT-670, Lakeshore) placed at the end of the cold head, and controlled with an accuracy ±0.2 K using a Lakeshore Model 325 temperature controller and two ceramic heaters (100 W).

Purified liquid H_2O (resistivity ≥18.2 MΩ cm at 298 K) was obtained from a Millipore Milli-Q water purification system and degassed by several freeze–pump–thaw cycles. The measurement of decoupled OD stretching vibrations of HDO molecules in the

[a] *Institute of Low Temperature Science, Hokkaido University, Sapporo, 060-0819, Japan. E-mail: hama@lowtem.hokudai.ac.jp*
[b] *Department of Chemistry, Graduate School of Science, Kyoto University, Kyoto, 606-8502, Japan*
[c] *Precursory Research for Embryonic Science and Technology (PRESTO), Japan Science and Technology Agency (JST), Saitama 332-0012, Japan*
[d] *Dipartimento di Fisica e Astronomia, Università di Catania, I-95125, Catania, Sicily, Italy*

† Electronic supplementary information (ESI) available. See DOI: 10.1039/c7cp03315j

H_2O ice employed purified H_2O liquid with 2.0 wt% (1.8 mol%) D_2O (deuteration degree >99.9%, Merck) to obtain a water sample containing about 3.5 mol% HDO with a negligible amount of D_2O. A mixture of water vapor and Ne gas (99.999%, Tokyo Gas Chemicals) or Ar gas (99.9999%, Koatsu Gas Kogyo) in a ratio of 1 : 1000 was introduced onto the substrate at 6 K through a capillary plate, typically for 30 min at 1×10^{-2} Pa. Since the conductance of the gas line should be different between H_2O and Ne (or Ar) gases, the actual matrix composition may be different from the premixed gas ratio. The pressure was measured using a cold cathode gauge (423 I-Mag® Cold Cathode Vacuum Sensor, MKS) and calculated using the gas correction factor for Ne (0.30). This approximately corresponds to an exposure of 6×10^{19} molecules cm^{-2}. For reference, there are about $2.0(1.4) \times 10^{15}$ molecules cm^{-2} on the surface of crystalline Ne(Ar), considering that there are four molecules in a unit cell with lattice parameters of a = 4.46(5.30) Å.[16,17] Hence, 6×10^{19} molecules cm^{-2} correspond to 30 000 (42 000) monolayers (ML) exposure, assuming 1 ML = $2.0(1.4) \times 10^{15}$ molecules cm^{-2}. The film thickness was roughly estimated to be about 7(11) μm.

The prepared H_2O/Ne matrix was warmed at a rate of 0.1 K s^{-1} to the desired temperature (10.5–13 K with an accuracy of ±1 K) to sublime the Ne matrix. The pressure in the main chamber was increased to the order of 10^{-1} Pa during sublimation of the Ne matrix. The time required for Ne matrix sublimation (and thus ice formation) is summarized in Table 1. The errors reflect fluctuations in temperature during heating in independent statistical experiments. At 10 K, Ne did not completely sublime even after 60 min. Samples were monitored *in situ* by FT-IR in reflection geometry (incident angle 83°) with a resolution of 2 cm^{-1} at a scan speed of 2 cm s^{-1} (Spectrum One, PerkinElmer). Spectra were accumulated 100 times (about 105 s) unless otherwise stated. Integrated IR intensities for the OH stretching vibration band of the ice samples obtained after Ne/Ar matrix sublimation were equivalent with an accuracy of ±10%.

Vapor-deposited H_2O ice was produced by the vapor deposition of water onto the substrate at 11 K through the capillary plate, typically for 7 min at 1×10^{-5} Pa. This corresponds to the exposure of approximately 2×10^{16} molecules cm^{-2}. Crystalline ice was produced by annealing the vapor-deposited amorphous ice from 11 K to 160 K and cooling it back to 11 K for IR measurements.

Table 1 Ne matrix sublimation time and averaged Ne sublimation rate at 10.5–13 K

Temperature (K)	Sublimation time (s)[a]	Averaged Ne sublimation rate (ML s^{-1})[b]
10.5	910 ± 86	33 ± 3
11	170 ± 84	233 ± 115
12	47 ± 8	667 ± 122
13	15 ± 1	2009 ± 134

[a] The time to reach the target temperature from 6 K (at heating rate of 0.1 K s^{-1}) is not counted due to the sufficiently low sublimation rate below 10.5 K. [b] We assume 30 000 ML of the Ne matrix, neglecting any sublimation of the Ne matrix during heating to the target temperature.

Experimental results

Fig. 1A shows the IR reflection–absorption spectrum of the OH stretching vibrational mode of H_2O monomers in the H_2O/Ne (1/1000) matrix at 6 K just after exposure of approximately 6×10^{19} molecules cm^{-2}. This scheme is well known in matrix isolation spectroscopy.[18–21] Given that H_2O monomers are almost freely rotating in the inert Ne matrix at 6 K, the IR spectrum shows rovibrational transitions.[18] H_2O dimers are evident at 3763 and 3590 cm^{-1},[19] as well as a small number of H_2O trimers at 3530 cm^{-1}.[20]

The H_2O/Ne matrix was then warmed at a rate of 0.1 K s^{-1} to 11 K. Fig. 1B shows transient single spectra of the H_2O/Ne matrix during heating to 11 K from 6 K. Fig. 1C shows 20 accumulated IR spectra measured after the H_2O/Ne matrix reached 11 K. These figures show that H_2O clusters (dimer to hexamer) had already formed above 9 K. These clusters were formed predominantly in the bulk matrix, because H_2O molecules can diffuse in a bulk Ne matrix above 9 K,[21] and the Ne atoms sublime sufficiently slowly below 10.5 K (Table 1).

Fig. 1D shows transient single spectra recorded during the Ne matrix sublimation at 11 K. The average Ne sublimation rate is 233 ± 115 ML s^{-1} (Table 1). The spectral shape clearly changes during the sublimation, as the monomers and clusters aggregated to form ice. The spectra measured at 38 and 78 s show a broad absorption peak at 3300–3400 cm^{-1}, indicating the formation of amorphous ice. The peak then gradually red-shifted in subsequent spectra (104–126 s), and the sharp crystalline feature denoting a four-coordinated tetrahedral hydrogen-bonding network later appeared at around 3230 cm^{-1} (150–196 s).[22–24]

Fig. 2 compares IR spectra measured at 11 K of the ice obtained after sublimation of the Ne matrix, vapor-deposited amorphous ice, and crystalline ice I. The samples were prepared using H_2O with 3.5 mol% HDO to allow measurement of the OD stretching vibration decoupled from intramolecular and intermolecular OH stretching vibrations,[25,26] because the peak frequency of its simple spectrum is sensitive to the local lattice structure (oxygen–oxygen distance) of the ice.[27–30] The OH spectrum of vapor-deposited amorphous ice shows a broad absorption feature with a peak at around 3400 cm^{-1} (Fig. 2A). This is remarkably different from the spectrum of the ice obtained after sublimation of the Ne matrix, which is clearly similar to that of crystalline ice.

In the decoupled OD stretching vibrational region (Fig. 2B), crystalline ice I shows a sharp single peak at 2414 cm^{-1}.[29] In contrast, vapor-deposited amorphous ice has a broad feature with a peak at 2450 cm^{-1}. The ice obtained after sublimation of the Ne matrix shows an OD spectrum with a peak at 2414 cm^{-1}, which is in agreement with that of crystalline ice I at 11 K. Other high-pressure phases of ice have peak frequencies generally blue-shifted from that of ice I due to the long oxygen–oxygen distances, which arise due to weak hydrogen bonds.[1,27–38] Clathrate hydrates also have peak frequencies different from those of ice I, depending on the guest–host interactions.[39–41] Hence, we conclude that the ice obtained after Ne matrix sublimation is crystalline ice I.

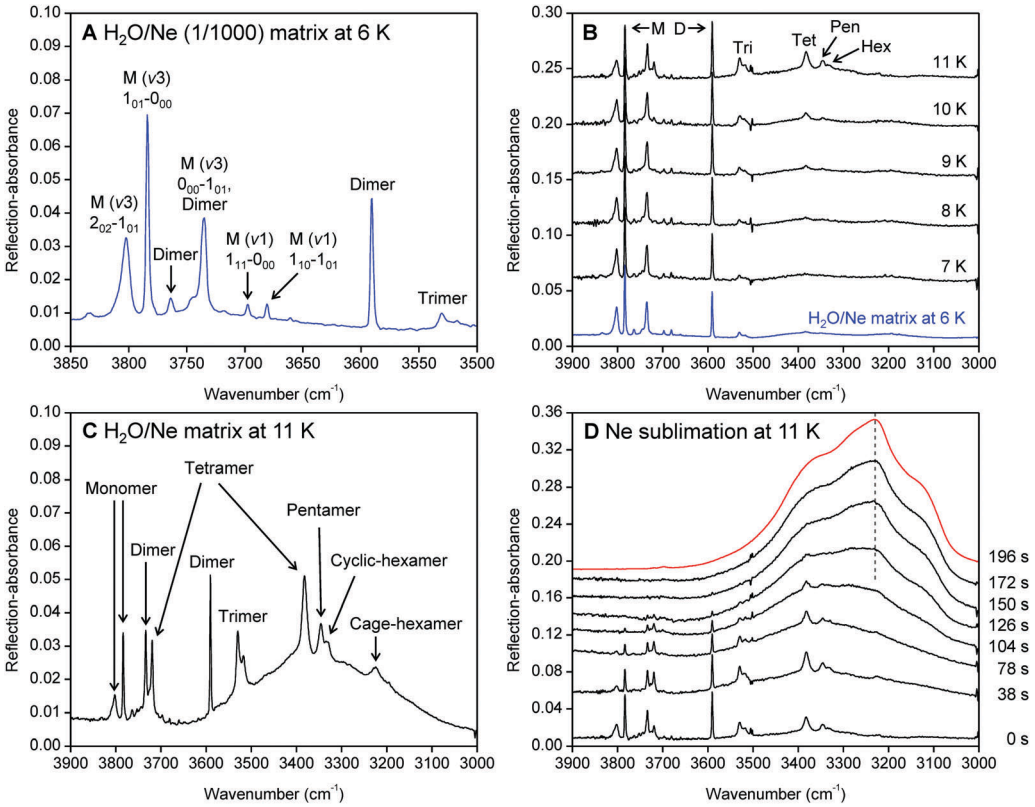

Fig. 1 Infrared reflection–absorption spectra in the OH stretching vibrational region. (A) H_2O in a Ne matrix (H_2O/Ne = 1/1000) at 6 K. M(ν3 or ν1) represents rovibrational transitions of the monomer in the ν3 and ν1 stretching mode, where indications $\left(J'_{K'_aK'_c} \leftarrow J_{K_aK_c}\right)$ are rotational assignments.[18] (B) Lower blue spectrum is the H_2O/Ne (1/1000) matrix at 6 K. Black spectra are transient single spectra during heating to 11 K from 6 K. M, D, Tri, Tet, Pen, and Hex represent monomer, dimer, trimer, tetramer, pentamer, and hexamer, respectively. (C) Twenty accumulated IR spectra measured after the H_2O/Ne matrix reached 11 K. The measurement time was 21 s. (D) Black lines are transient single spectra during sublimation of the Ne matrix at 11 K. The upper red line is for the ice obtained after Ne matrix sublimation at 11 K. The dashed gray guideline is at 3230 cm^{-1}. The assignment is based on the references.[18–21]

Note that IR spectroscopy cannot distinguish between I_h and I_c.[1,27] The small shoulder appearing at a high wavenumber suggests a minor amount of amorphous ice.

We also found that the ice became amorphous, rather than crystalline, at 13 or 10.5 K (Fig. 3). Typical times for Ne sublimation are 15 ± 1 s (2009 ± 134 ML s^{-1}) at 13 K and 910 ± 86 s (33 ± 3 ML s^{-1}) at 10.5 K (Table 1). Although the OH spectra at 13 K and 10.5 K have a peak at 3270 cm^{-1}, there is no clear peak at around 3230 cm^{-1} (Fig. 3A). The peak at 3270 cm^{-1} has been ascribed to four-coordinated water molecules with a distorted tetrahedral structure.[22–24] The OD spectral shapes are sharper and red-shifted compared with that of the vapor-deposited amorphous ice (Fig. 2B and 3B). However, the 2414 cm^{-1} crystalline peak is weaker at 10.5 K than that at 11–12 K, and it is absent at 13 K. Because the OD-stretch frequency red-shifts as strong hydrogen bonds with short lattice distances are formed,[25,26] these results indicate that the ices formed at 10.5 and 13 K are predominantly amorphous, but they have stronger hydrogen-bonding networks than the vapor-deposited amorphous ice (Fig. S1, ESI†). Crystalline ice formed only at 11–12 K, when the sublimation time was in the range of 39–254 s (118–789 ML s^{-1}) (Table 1). The temperature dependence shows that unique molecular dynamics occur during the sublimation of Ne and that the sublimation rate has a key influence on the lattice structure of ice.

For further elucidating the crystalline ice formation mechanism, we performed experiments using a water/argon (H_2O/Ar = 1/1000) matrix prepared at 6 K (Fig. 4). We found that the ice became amorphous, even when the average Ar matrix sublimation rate is 412 ML s^{-1} at 46 K, corresponding to an intermediate sublimation rate of the Ne matrix for the crystalline ice formation at 11–12 K (118–789 ML s^{-1}, Table 1).

Fig. 4A shows the IR spectrum of an H_2O/Ar (1/1000) matrix at 6 K.[18,42,43] The number of H_2O dimers appears to be smaller than that in the H_2O/Ne matrix (Fig. 1A).[19] In addition, the reflection–absorbance intensity was weaker in the Ar matrix than in the Ne matrix (Fig. 1). These differences can arise from the thickness difference between the Ar (42 000 ML, 11 μm) and Ne (30 000 ML, 7 μm) matrices assuming the same amount of exposure (6×10^{19} molecules cm^{-2}): the number density of H_2O molecules can become small in a thick sample, and the IR reflection–absorbance intensity strongly depends on film thickness due to optical interference effects.[44] Fig. 4B shows transient single spectra of the H_2O/Ar matrix during heating to 46 K from 6 K at a rate of 0.2 K s^{-1}. These spectra show that most of the H_2O monomers had already been aggregated to

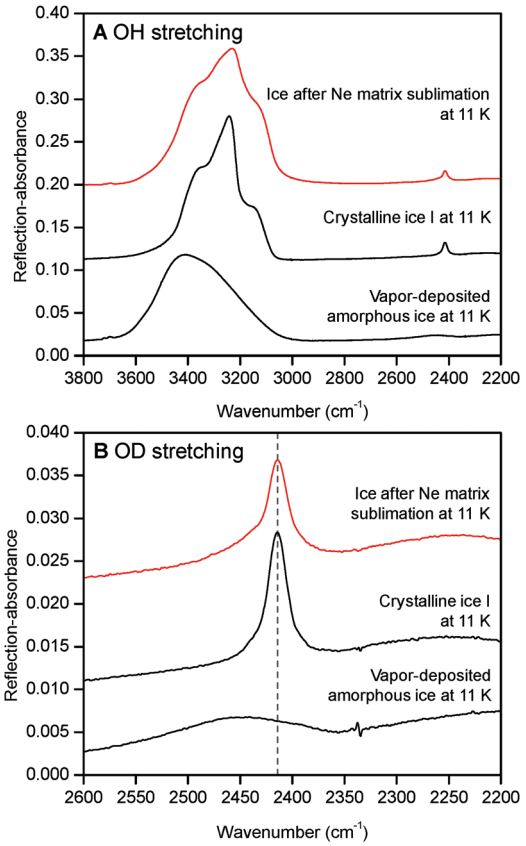

Fig. 2 Infrared reflection–absorption spectra of ice after Ne matrix sublimation, vapor-deposited amorphous ice, and crystalline ice I. (A) OH stretching vibrational region. (B) OD stretching vibrational region. The ice samples were prepared using H_2O with 3.5 mol% HDO. The dashed gray guideline is at 2414 cm^{-1}.

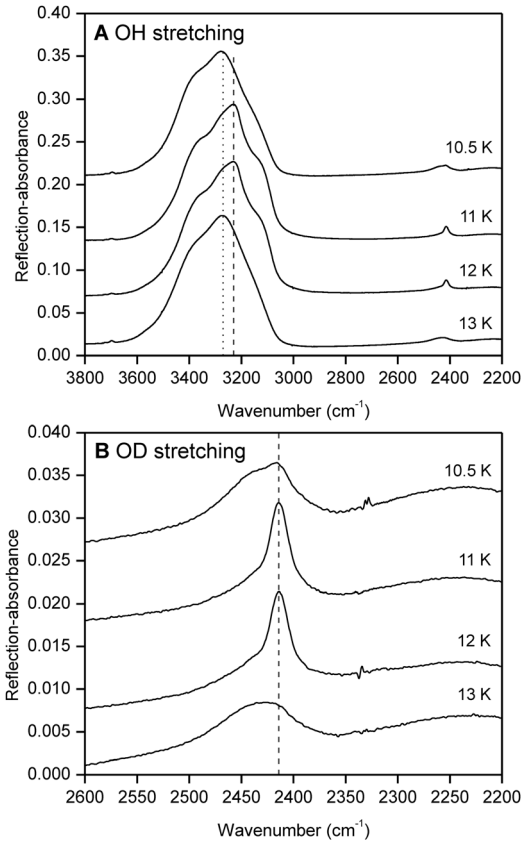

Fig. 3 Infrared reflection–absorption spectra of ice obtained after Ne matrix sublimation at 10.5–13 K using H_2O with 3.5 mol% HDO. (A) OH stretching vibrational region. The dotted and dashed gray guidelines are at 3270 and 3230 cm^{-1}, respectively. (B) OD stretching vibrational region. The dashed gray guideline is at 2414 cm^{-1}.

form water clusters in the bulk of the Ar matrix before reaching 46 K.[19–21,45] This is different from the H_2O/Ne matrix at 11 K, in which a substantial amount of H_2O monomers still remains (Fig. 1B). Water clusters larger than a hexamer were evident at 3140 cm^{-1} in the H_2O/Ar matrix at 46 K (Fig. 4C).[21]

Fig. 4D shows transient single spectra recorded during the Ar matrix sublimation at 46 K. Further aggregation of these water clusters eventually resulted in the formation of amorphous ice. The OH spectrum has a peak at 3306 cm^{-1} after sublimation of the Ar matrix (102 s). In the decoupled OD stretching vibrational region (Fig. 5), the ice has a broad feature with a peak at 2446 cm^{-1}, but lacks the 2414 cm^{-1} crystalline peak. The formation of amorphous ice has also been observed in our previous study using the sublimation of a CO matrix (H_2O/CO = 1/50), in which most of the H_2O molecules were also aggregated in the bulk of the CO matrix during heating to 35 K from 10 K.[14] These results suggest that once large water clusters and amorphous ices were formed in the matrix, they cannot attain a crystalline configuration by structural rearrangement during further aggregation. Crystalline ice formation at 11–12 K can mainly occur through the aggregation of water monomers and/or small clusters on the sublimating surface of the solid Ne.

Discussion

We discuss below the formation conditions of crystalline/amorphous ice, focusing on the mobility of H_2O molecules.[7] The formation of crystalline ice requires water molecules to settle on the energetically most-favorable sites. They must therefore be able to diffuse to a suitable site before new monomers are adsorbed and molecular motion ceases.[7] For this to occur, the surface diffusion coefficient, D_s (cm^2 s^{-1}), multiplied by the time taken to cover the surface by adsorbed water molecules, t_{cover} (s), must be greater than the lattice site area of the crystalline ice, a_{ice}^2 (cm^2).[7]

$$D_s\, t_{cover} > a_{ice}^2, \quad (1)$$

where a_{ice} is the lattice parameter of the crystalline ice. The surface diffusivity of H_2O molecules on solid Ne (*e.g.*, on the surface of the Ne matrix subliming here) differs greatly from that on water ice (*e.g.*, from vapor deposition). The van der Waals interaction between an H_2O molecule and a Ne atom is 0.80 kJ mol^{-1} (96 K), which is slightly stronger than that of a Ne–Ne dimer (0.35 kJ mol^{-1}, 42 K) and much weaker than the hydrogen-bond strength for the H_2O–H_2O dimer (20.8 kJ mol^{-1},

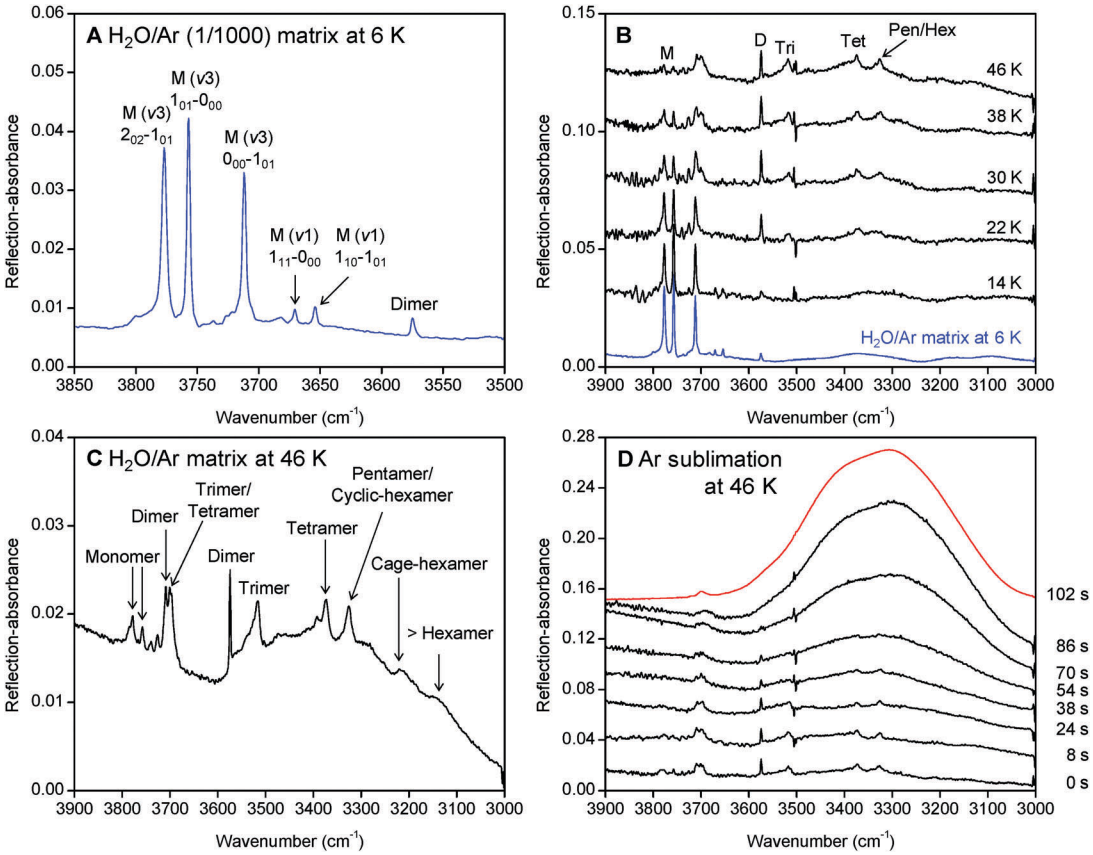

Fig. 4 Infrared reflection–absorption spectra in the OH stretching vibrational region. (A) H_2O in an Ar matrix (H_2O/Ar = 1/1000) at 6 K. M(ν3 or ν1) represents rovibrational transitions of the monomer in the ν3 and ν1 stretching mode, where indications $\left(J'_{K'_a K'_c} \leftarrow J_{K_a K_c}\right)$ are rotational assignments.[18,42,43] (B) Lower blue spectrum is the H_2O/Ar (1/1000) matrix at 6 K. Black spectra are transient single spectra during heating to 46 K from 6 K. M, D, Tri, Tet, Pen, and Hex represent monomer, dimer, trimer, tetramer, pentamer, and hexamer, respectively. (C) Twenty accumulated IR spectra measured after the H_2O/Ar matrix reached 46 K. The measurement time was 21 s. (D) Black lines are transient single spectra during sublimation of the Ar matrix at 46 K. The upper red line is for the ice obtained after Ar matrix sublimation at 46 K. The assignment is based on the references.[19–21,45]

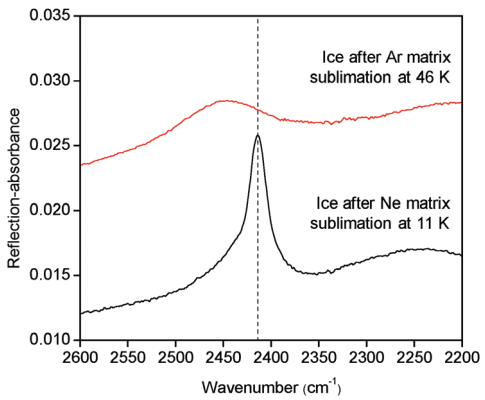

Fig. 5 Infrared reflection–absorption spectra of ices after Ar matrix sublimation at 46 K and after Ne matrix sublimation at 11 K in the OD stretching vibrational region. The ice samples were prepared using H_2O with 3.5 mol% HDO. The time required for the Ar matrix sublimation is 152 s. The dashed gray guideline is at 2414 cm^{-1}.

2510 K).[46–48] The D_s of H_2O on solid Ne can be estimated by means of the Arrhenius equation:

$$D_s = \nu\, a^2 \exp(-E_s/k_B T), \quad (2)$$

where ν, a, E_s, k_B, and T are the frequency factor (typically 10^{12} s^{-1}),[49] a lattice parameter, the surface diffusion barrier, the Boltzmann constant, and temperature, respectively. Adopting the lattice parameter of crystalline Ne (*i.e.*, a = 4.46 Å), with 0.80 kJ mol^{-1} for E_s,[16,46] gives a value of $D_s = 3.2 \times 10^{-7}$ cm^2 s^{-1} at 11 K. This value is 95 orders of magnitude larger than that of H_2O on ice at 11 K ($D_s = 2.2 \times 10^{-102}$ cm^2 s^{-1}), and is still three orders of magnitude larger than that of H_2O on ice even at 160 K (3.2×10^{-10} cm^2 s^{-1}), as calculated using the lattice parameter of ice I (4.50 Å) and E_s = 20.8 kJ mol^{-1}.[48,50] Although rigorous calculations for the D_s of H_2O on solid Ne and ice must consider many-body effects, these values imply that H_2O molecules can rapidly diffuse on solid Ne at 11 K. Hence, we suggest that H_2O molecules in a subliming Ne matrix can attain a stable configuration when they meet the water ice on the solid Ne before they are immobilized by the creation of hydrogen bonds (Fig. 6).

This process can also qualitatively explain the effect of temperature on the resulting ice structure. At 13 K, the rapid Ne sublimation (15 ± 1 s, 2009 ± 134 ML s^{-1}) would make t_{cover}

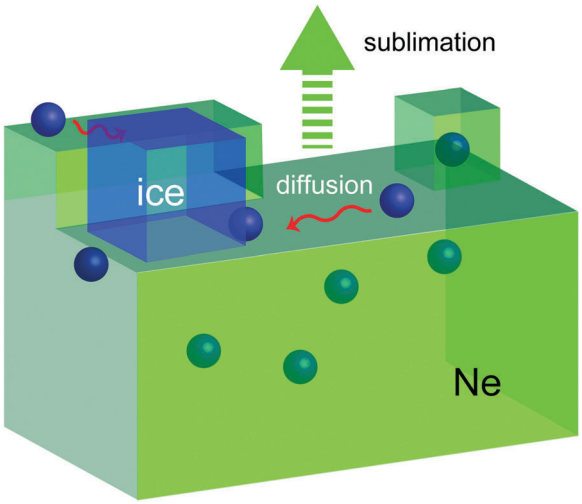

Fig. 6 Schematic of water ice formation by Ne matrix sublimation.

too short to allow H_2O molecules to settle in crystalline configurations. At 10.5 K, water molecules would mainly aggregate in the bulk of the Ne matrix rather than on the subliming surface, owing to the slow sublimation rate of Ne at this temperature (910 ± 86 s, 33 ± 3 ML s^{-1}) and to the non-negligible diffusivity of water molecules in the bulk Ne matrix above 9 K.[21] However, the bulk diffusivity is much lower than that at the surface,[51,52] and this is likely to prevent water molecules from attaining a crystalline configuration below 10.5 K. In fact, the formation of amorphous ice was confirmed in the experiments using the H_2O/Ar (1/1000) matrix, where the aggregation of water monomers mainly occurs in the bulk of the Ar matrix before reaching the sublimation temperature of 46 K (Fig. 4 and 5).

It should be noted that, in the early stages of Ne sublimation at 11 K, amorphous ice forms mainly by the aggregation of water molecules (0–104 s, Fig. 1D). We also confirmed that only amorphous ice is formed at 11 K when the initial thickness of the H_2O/Ne matrix is decreased. Fig. 7 shows IR reflection–absorption spectra of the ice obtained after Ne matrix sublimation at 11 K with different exposures (1.5–6.0 × 10^{19} molecules cm^{-2}) using H_2O with 3.5 mol% HDO. The OH and decoupled OD stretching vibrational regions are shown in Fig. 7A and B, respectively. Fig. 7C shows the dangling OH stretching vibrational region, for reference. Because the times required for the Ne matrix sublimation at 11 K almost linearly increased with increasing gas exposure (Fig. 7D), there was no thermal

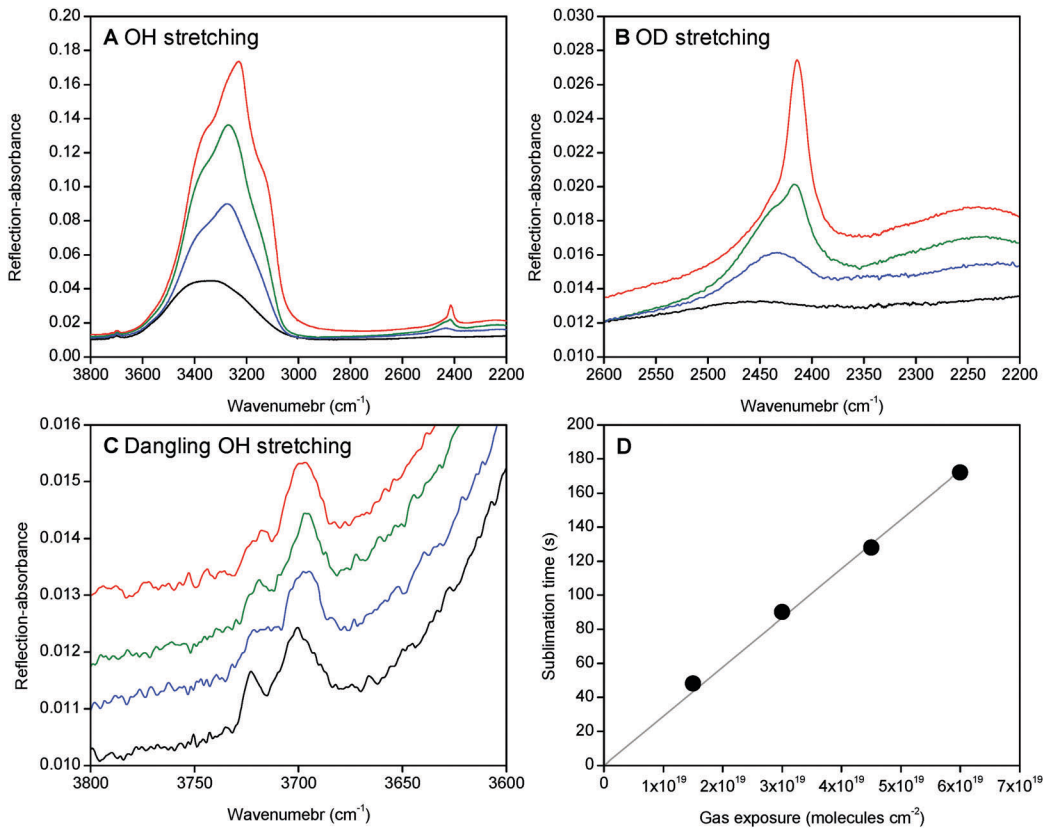

Fig. 7 Infrared reflection–absorption spectra of ices obtained after Ne matrix sublimation at 11 K with different exposures (1.5–6.0 × 10^{19} cm^{-2}) using H_2O with 3.5 mol% HDO, for (A) OH stretching, (B) decoupled OD stretching, and (C) dangling OH stretching vibrational regions, in which the exposure of the H_2O/Ne (1/1000) gas is approximately 1.5 × 10^{19} molecules cm^{-2} (black), 3.0 × 10^{19} molecules cm^{-2} (blue), 4.5 × 10^{19} molecules cm^{-2} (green), and 6.0 × 10^{19} molecules cm^{-2} (red). (D) Plots of the times required for the Ne matrix sublimation as function of gas exposure: 48 s (1.5 × 10^{19} molecules cm^{-2}), 90 s (3.0 × 10^{19} molecules cm^{-2}), 128 s (4.5 × 10^{19} molecules cm^{-2}), and 172 s (6.0 × 10^{19} molecules cm^{-2}). The gray guideline is a linear fit for reference.

gradient across the H_2O/Ne matrix in each thickness experiment. The exposure of the H_2O/Ne gas less than 3.0×10^{19} molecules cm^{-2} led both the OH and OD stretching vibrational spectra to show broad absorption features, indicating the formation of amorphous ice at 11 K. This thickness dependence of the resulting ice structures suggests that long-range ordered crystalline ice formation takes place after the formation of amorphous ice, which is consistent with the transient single spectra during Ne matrix sublimation at 11 K in Fig. 1D. These results suggest the size dependence of the stable configuration of water ice: the thermodynamically lowest-energy lattice structure is amorphous for the initially formed small ice aggregates. In good agreement with our results, previous studies have reported that for small water clusters, typically $n < 200$, the amorphous structure is energetically more stable than a crystalline, long-range ordered tetrahedral network.[22–24] The sublimation of the thick Ne matrix (by refreshing the surface) would allow the ice to grow a long-range ordered crystalline structure from the surface of a sufficiently large amorphous ice on the solid Ne.

Finally, the dangling OH bonds are briefly discussed. Fig. 7C shows two small peaks assigned to the dangling OH bonds at around 3720 and 3698 cm^{-1}. These peaks are assigned to two- and three-coordinated H_2O molecules, respectively.[53–55] The signal intensities of the dangling OH bonds were almost constant in the ices with different exposures ($1.5–6.0 \times 10^{19}$ molecules cm^{-2}). This indicates that the dangling OH bonds should be mainly attributed to the microporous structure of amorphous ice formed in the early stages of Ne sublimation. The crystalline ice subsequently formed on the amorphous ice would have a compact structure with a low concentration of dangling OH bonds.

A molecular-level understanding of the crystalline ice formation at 11–12 K will require a more detailed future investigation. In addition to FT-IR, diffraction studies are also highly desirable to elucidate the formation of ice I_h, I_c, or stacking disordered ice I (ice I_{sd}),[56–58] as well as the possible presence of clathrate hydrates. Previous studies examining clathrate hydrates have reported that molecular transport is promoted by the presence of defects in the structure.[39–41,59] Theoretical studies show the dependence of clathrate-hydrate formation rates on the abundance and mobility of vacancy/interstitial defects rather than orientational (Bjerrum) defects.[41,59] In the present study, the amorphous ice formed in the early stages of Ne sublimation can have a high population of vacancy/interstitial defects, as suggested by the presence of the dangling OH bonds (Fig. 7). This can promote the mobility of the H_2O molecules at the ice surface during further aggregation on the solid Ne, and trigger the crystalline ice formation at 11–12 K. Evaluation of the role of defects in the observed low-temperature crystalline ice formation awaits molecular dynamics simulations.

Conclusions

We have demonstrated the possibility of crystalline-ice formation at an extremely low temperature of 11–12 K through Ne sublimation from a solid H_2O/Ne (1/1000) matrix, which is much colder than the traditionally believed temperature of crystalline-ice formation. Our results show a novel crystal formation mechanism; that is, the molecules in a weakly interacting system can be sufficiently mobile to overcome the kinetic barrier to form crystals even at extremely low temperature.

Acknowledgements

We thank H. Hidaka, Y. Oba, K. K. Tanaka, T. Lamberts, S. Enami, T. Shimoaka, and T. Hasegawa for helpful comments and discussions. This work was supported by Japan Society for the Promotion of Science Grants-in-Aid for Scientific Research 24224012 and 16H06024, and Ministry of Education, Culture, Sports, Science and Technology Grant-in-Aid for Scientific Research 25108002, and 16H00937. The authors declare no conflicts of interest.

Notes and references

1 C. G. Salzmann, P. G. Radaelli, B. Slater and J. L. Finney, *Phys. Chem. Chem. Phys.*, 2011, **13**, 18468–18480.
2 A. Falenty, T. C. Hansen and W. F. Kuhs, *Nature*, 2014, **516**, 231–233.
3 E. F. Burton and W. F. Oliver, *Nature*, 1935, **135**, 505–506.
4 E. F. Burton and W. F. Oliver, *Proc. R. Soc. A*, 1935, **153**, 166–172.
5 T. Bartels-Rausch, V. Bergeron, J. H. E. Cartwright, R. Escribano, J. L. Finney, H. Grothe, P. J. Gutiérrez, J. Haapala, W. F. Kuhs, J. B. C. Pettersson, S. D. Price, C. Ignacio Sainz-Díaz, D. J. Stokes, G. Strazzulla, E. S. Thomson, H. Trinks and N. Uras-Aytemiz, *Rev. Mod. Phys.*, 2012, **84**, 885–944.
6 T. Loerting, K. Winkel, M. Seidl, M. Bauer, C. Mitterdorfer, P. H. Handle, C. G. Salzmann, E. Mayer, J. L. Finney and D. T. Bowron, *Phys. Chem. Chem. Phys.*, 2011, **13**, 8783–8794.
7 A. Kouchi, T. Yamamoto, T. Kozasa, T. Kuroda and J. M. Greenberg, *Astron. Astrophys.*, 1994, **290**, 1009–1018.
8 P. Jenniskens and D. Blake, *Astrophys. J.*, 1996, **473**, 1104–1113.
9 Z. Dohnalek, G. A. Kimmel, R. L. Ciolli, K. P. Stevenson, R. Scott Smith and B. D. Kay, *J. Chem. Phys.*, 2000, **112**, 5932–5941.
10 *The Science of Solar System Ices*, ed. M. S. Gudipati and J. Castillo-Rogez, Springer, New York, 2013.
11 T. Hama and N. Watanabe, *Chem. Rev.*, 2013, **113**, 8783–8839.
12 A. C. A. Boogert, P. A. Gerakines and D. C. B. Whittet, *Annu. Rev. Astron. Astrophys.*, 2015, **53**, 541–581.
13 K. Kuwahata, T. Hama, A. Kouchi and N. Watanabe, *Phys. Rev. Lett.*, 2015, **115**, 133201.
14 A. Kouchi, T. Hama, Y. Kimura, H. Hidaka, R. Escribano and N. Watanabe, *Chem. Phys. Lett.*, 2016, **658**, 287–292.
15 T. Hama, H. Ueta, A. Kouchi and N. Watanabe, *Proc. Natl. Acad. Sci. U. S. A.*, 2015, **112**, 7438–7443.
16 D. N. Batchelder, D. L. Losee and R. O. Simmons, *Phys. Rev.*, 1967, **162**, 767–775.

17 O. G. Peterson, D. N. Batchelder and R. O. Simmons, *Phys. Rev.*, 1966, **150**, 703–711.
18 D. Forney, M. E. Jacox and W. E. Thompson, *J. Mol. Spectrosc.*, 1993, **157**, 479–493.
19 J. Ceponkus, P. Uvdal and B. Nelander, *J. Chem. Phys.*, 2010, **133**, 74301.
20 J. Ceponkus, P. Uvdal and B. Nelander, *J. Chem. Phys.*, 2011, **134**, 64309.
21 J. Ceponkus, P. Uvdal and B. Nelander, *J. Phys. Chem. A*, 2012, **116**, 4842–4850.
22 V. Buch, B. Sigurd, J. P. Devlin, U. Buck and J. K. Kazimirski, *Int. Rev. Phys. Chem.*, 2004, **23**, 375–433.
23 C. C. Pradzynski, R. M. Forck, T. Zeuch, P. Slaví and U. Buck, *Science*, 2012, **337**, 1529–1532.
24 U. Buck, C. C. Pradzynski, T. Zeuch, J. M. Dieterich and B. Hartke, *Phys. Chem. Chem. Phys.*, 2014, **16**, 6859–6871.
25 F. Li and J. L. Skinner, *J. Chem. Phys.*, 2010, **132**, 204505.
26 F. Li and J. L. Skinner, *J. Chem. Phys.*, 2010, **133**, 244504.
27 J. E. Bertie and E. Whalley, *J. Chem. Phys.*, 1964, **40**, 1637–1645.
28 J. E. Bertie and E. Whalley, *J. Chem. Phys.*, 1964, **40**, 1646–1659.
29 *Water a Comprehensive Treatise*, Water and Aqueous Solutions at Subzero Temperatures, ed. F. Franks, Plenum Press, New York, 1972, vol. 7.
30 *Water Science Reviews 2*, ed. F. Franks, Cambridge University Press, 1986, vol. 2.
31 B. Minceva-Sukarova, W. F. Sherman and G. R. Wilkinson, *J. Phys. C: Solid State Phys.*, 1984, **17**, 5833–5850.
32 C. G. Salzmann, A. Hallbrucker, J. L. Finney and E. Mayer, *Chem. Phys. Lett.*, 2006, **429**, 469–473.
33 T. F. Whale, S. J. Clark, J. L. Finney and C. G. Salzmann, *J. Raman Spectrosc.*, 2013, **44**, 290–298.
34 C. Salzmann, P. G. Radaelli, A. Hallbrucker, E. Mayer and J. L. Finney, *Science*, 2007, **311**, 1758–1761.
35 C. Salzmann, I. Kohl, T. Loerting, E. Mayer and A. Hallbrucker, *J. Phys. Chem. B*, 2003, **107**, 2802–2807.
36 C. Salzmann, I. Kohl, T. Loerting, E. Mayer and A. Hallbrucker, *J. Phys. Chem. B*, 2002, **106**, 1–6.
37 J. J. Shephard, S. Klotz and C. G. Salzmann, *J. Chem. Phys.*, 2016, **144**, 204502.
38 D. D. Klug and E. Whalley, *J. Chem. Phys.*, 1984, **81**, 1220–1228.
39 P. J. Wooldridge, H. H. Richardson and J. P. Devlin, *J. Chem. Phys.*, 1987, **87**, 4126–4131.
40 J. P. Devlin and I. A. Monreal, *Chem. Phys. Lett.*, 2010, **492**, 1–8.
41 V. Buch, J. P. Devlin, I. A. Monreal, B. Jagoda-Cwiklik, N. Uras-Aytemiz and L. Cwiklik, *Phys. Chem. Chem. Phys.*, 2009, **11**, 10245–10265.
42 X. Michaut, A.-M. Vasserot and L. Abouaf-Marguin, *Vib. Spectrosc.*, 2004, **34**, 83–93.
43 R. Sliter, M. Gish and A. F. Vilesov, *J. Phys. Chem. A*, 2011, **115**, 9682–9688.
44 B. D. Teolis, M. J. Loeffler, U. Raut, M. Famá and R. A. Baragiola, *Icarus*, 2007, **190**, 274–279.
45 J. Ceponkus, G. Karlström and B. Nelander, *J. Phys. Chem. A*, 2005, **109**, 7859–7864.
46 M. P. Hodges, R. J. Wheatley and A. H. Harvey, *J. Chem. Phys.*, 2002, **117**, 7169–7179.
47 R. J. Gdanitz, *Chem. Phys. Lett.*, 2001, **348**, 67–74.
48 A. Hodgson and S. Haq, *Surf. Sci. Rep.*, 2009, **64**, 381–451.
49 E. R. Batista and H. Jónsson, *Comput. Mater. Sci.*, 2001, **20**, 325–336.
50 K. Röttger, A. Endriss, J. Ihringer, S. Doyle and W. F. Kuhs, *Acta Crystallogr., Sect. B: Struct. Sci.*, 1994, **50**, 644–648.
51 S. Nie, N. C. Bartelt and K. Thürmer, *Phys. Rev. Lett.*, 2009, **102**, 136101.
52 D. E. Brown and S. M. George, *J. Phys. Chem.*, 1996, **100**, 15460.
53 V. Buch and J. P. Devlin, *J. Chem. Phys.*, 1991, **94**, 4091–4092.
54 B. Rowland and J. P. Devlin, *J. Chem. Phys.*, 1991, **94**, 812–813.
55 M. A. Zondlo, T. B. Onasch, M. S. Warshawsky, M. A. Tolbert, G. Mallick, P. Arentz and M. S. Robinson, *J. Phys. Chem. B*, 1997, **101**, 10887–10895.
56 T. H. G. Carr, J. J. Shephard and C. G. Salzmann, *J. Phys. Chem. Lett.*, 2014, **5**, 2469–2473.
57 W. F. Kuhs, C. Sippel, A. Falenty and T. C. Hansen, *Proc. Natl. Acad. Sci. U. S. A.*, 2012, **109**, 21259–21264.
58 T. L. Malkin, B. J. Murray, C. G. Salzmann, V. Molinero, S. J. Pickering and T. F. Whale, *Phys. Chem. Chem. Phys.*, 2015, **17**, 60–76.
59 A. Demurov, R. Radhakrishnan and B. L. Trout, *J. Chem. Phys.*, 2002, **116**, 702–709.

